

Fractionalization of a flux quantum in a one-dimensional parallel Josephson junction array with alternating π junctions

Mahesh Chandran^{1*} and R. V. Kulkarni^{2†}

¹*Tata Institute of Fundamental Research, Homi Bhabha Road, Mumbai, 400 005, INDIA.*

²*Department of Physics, University of California, Davis, CA 95616.‡*

(Dated: November 13, 2018)

We study numerically and analytically the properties of a one-dimensional array of parallel Josephson junctions in which every *alternate* junction is a π junction. In the ground state of the array, each cell contains spontaneous magnetic flux $\Phi \leq \Phi_0/2$ which shows *antiferromagnetic* ordering along the array. We find that an externally introduced 2π -fluxon Φ_0 in such an array is unstable and fractionalizes into two π fluxons of magnitude $\frac{1}{2}\Phi_0$. We attribute this fractionalization to the degeneracy of the ground state of the array. The magnitude of the flux in the fractional fluxons can be controlled by changing the critical current of the π junctions relative to the 0 junctions. In the presence of an external current, the fluxon lattice in the antiferromagnetic ground state can be depinned. We also observe a novel resonant structure in the V - I characteristics above the depinning current due to the interaction between the fluxon lattice and the array.

PACS numbers: 74.81.Fa, 75.10.Pq

One of the exciting developments in the field of Josephson devices is the fabrication of the three terminal controllable Josephson junction [1]. The supercurrent through a Josephson junction is given by $I = I_c \sin(\Delta\phi)$ where $\Delta\phi$ is the gauge-invariant phase difference between the superconductors, and the critical current I_c depends upon the junction geometry, normal state resistance R_n and the temperature T . Morpurgo *et al.*[1] showed that the supercurrent through a superconductor-metal-superconductor (SNS) junction changes on passing a control current through the normal metal. For such a junction, the supercurrent $I \propto \sin(\Delta\phi + \chi)$ where the additional phase difference χ is dependent on the current through the normal metal. Further theoretical work showed that in the diffusive limit of the junction, the additional phase factor χ can be made π , thus reversing the direction of the supercurrent with respect to the phase difference $\Delta\phi$ [2, 3]. Josephson junction with $\chi = \pi$ is referred as the π junction (we use the term 0 junction for the Josephson junction for which $\chi = 0$). The π junction has now been realized in several experiments [4, 5, 6]. The fabrication of such tunable junctions has opened immense possibilities for new applications, as demonstrated recently by the development of controllable π -SQUID [7].

The next natural step in this field would be to consider Josephson junction array (JJA) containing π junctions. Theoretically, Kusmartsev [8] considered a loop containing an odd number of π junctions and showed that the loop contains spontaneous magnetic flux in the ground state. In the continuum limit, the long Josephson junction with alternating critical current density have been studied which shows self-generated magnetic flux [9, 10]. Recent studies of JJAs with π junctions [11, 12] have shown some novel features arising out of the interplay between 0 and π junctions. Moreover, JJA is a unique system which provides experimental realizations of sev-

eral interesting physical phenomena, some examples of which are field induced superconductor to insulator transition [13], Aharonov-Casher effect [14], coherent emission of radiation [15]. One is then led to ask as what new physical phenomenon exist in the 1D JJA containing π junctions.

In this paper, we study numerically and analytically a new class of 1D JJA: an array of parallel Josephson junctions in which every *alternate* junction is a π junction. The ground state contains spontaneous magnetic flux in each cell and are ordered *antiferromagnetically* along the array. We find that a quantum of flux (fluxon) with a 2π kink in the phase is unstable in such an array, and fractionalizes into two spatially separated π kink fluxons. We also calculate the V - I characteristics which shows a novel structure due to resonant interaction between the moving antiferromagnetic fluxon lattice and the linear waves emitted by the array.

Consider a 1D array of parallel Josephson junctions containing alternate π - and 0 junctions (see inset Fig. 1). The Hamiltonian for this system is

$$\frac{H}{E_J} = \sum_{i=0}^{N-1} \frac{1}{2} \left(\frac{\partial \phi_i}{\partial t} \right)^2 + \frac{\lambda_J^2}{2} (\phi_{i+1} - \phi_i)^2 + [1 - (-1)^i \cos \phi_i], \quad (1)$$

where ϕ_i is the gauge-invariant phase difference across the i -th junction. The periodic boundary condition is imposed at the two ends of the array such that $\phi_0 = \phi_N$ (N is assumed to be even). In Eq.(1), the first term represents the charging energy and the second term is the energy of the induced magnetic field due to finite self-inductance of the cell (the effect of mutual inductance between the cells is neglected). The last term represents the energy associated with the Josephson currents. The prefactor for the $\cos \phi_i$ term alternates in sign for odd (π -) and even (0-) junctions. The Josephson coupling energy $E_J = I_c \Phi_0 / 2\pi$ where I_c is the critical current of

a single junction. The time t is in the units of inverse plasma frequency $\omega_P^{-1} = \sqrt{\frac{\Phi_0 C}{2\pi I_c}}$, where C is the averaged capacitance per unit area of the junction. The effective Josephson penetration depth is given by $\lambda_J = (\frac{\Phi_0}{2\pi L_0 I_c})^{1/2}$ where L_0 is the self inductance of a single cell. The λ_J determines the screening strength of the array, and is related to the SQUID parameter $\beta_L = \lambda_J^{-2}$.

From Eq.(1), the equation of motion for ϕ_i is

$$\frac{d^2\phi_i}{dt^2} + \alpha \frac{d\phi_i}{dt} + (-1)^i \sin \phi_i + \gamma = \lambda_J^2 (\phi_{i+1} + \phi_{i-1} - 2\phi_i), \quad (2)$$

where a dissipative term $\alpha \frac{d\phi_i}{dt}$ is also added [16]. The coefficient $\alpha = \beta_c^{-1/2}$, where $\beta_c = 2\pi R_n^2 I_c C / \Phi_0$ is the McCumber parameter. The parameter $\gamma = I_{ext} / I_c$ represents the external current through the junction. For the numerical simulation, Eq.(2) is integrated using the fourth order predictor-corrector method. The consistency of the steady state solutions was checked using different initial configurations of ϕ_i 's. The magnetic flux in the i^{th} cell is defined as $2\pi \frac{\Phi_i}{\Phi_0} = -(\phi_{i+1} - \phi_i)$. We remark that for the case where all junctions are 0 junctions (henceforth referred to as the 0-JJA), Eq.(2) is the discrete perturbed sine-Gordon equation, and have been studied extensively [17, 18]. First, we consider the results from the numerical simulation.

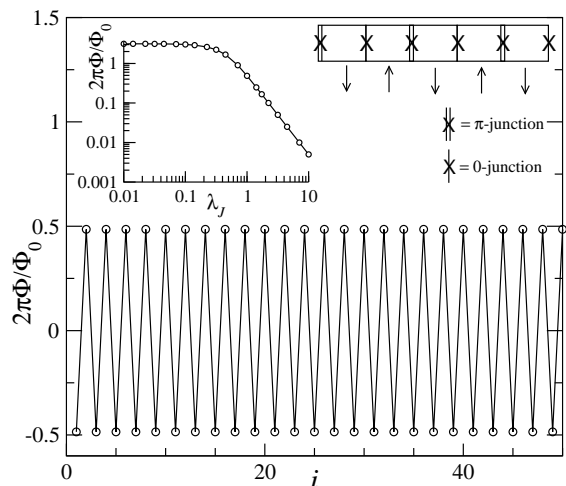


FIG. 1: The self-induced magnetic flux $2\pi\Phi_i/\Phi_0$ along the array in the ground state. The $\lambda_J = 1.0$ and $N = 100$ (only half the array is shown for clarity). The right inset shows the array geometry and the arrows represents the antiferromagnetic ordering of the magnetic flux induced in the cell. The left inset shows the dependence of $2\pi \frac{|\Phi_i|}{\Phi_0}$ on λ_J .

Figure 1 shows the ground state flux configuration $2\pi\Phi_i/\Phi_0$ for $N = 100$ and $\lambda_J = 1.0$. The self-induced magnetic flux Φ_i changes sign across neighboring cells with $|\Phi_i| = \Phi$ remaining constant. Such a configuration of Φ_i is reminiscent of the ground state in 1D classical Ising model with *antiferromagnetic* (AF) coupling, as depicted schematically in the inset of Fig. 1. Therefore,

we call this array the antiferromagnetic JJA (AFJJA). The AF ordering of Φ_i (and hence, ϕ_i) implies that the self-induced screening currents in neighboring cells are oppositely oriented. The magnitude of the flux Φ in a cell depends on the screening strength λ_J as shown in the Fig. 1(inset). With increasing λ_J , the magnetic flux in the neighboring cells tends to overlap, and $\Phi \rightarrow 0$ as $\lambda_J \rightarrow \infty$. In the strong screening limit, $\lambda_J \rightarrow 0$ and $\Phi \rightarrow \frac{\Phi_0}{2}$.

Next, we consider the consequence of introducing an external fluxon in AFJJA[19]. In the 0-JJA, a fluxon corresponds to a 2π -kink in the phase profile $\phi(x)$ and the magnetic field ($\propto \frac{\Delta\phi}{\Delta x}$) is spatially localized on the length scale λ_J . Figure 2(a) shows the steady state profiles of $2\pi\Phi_i/\Phi_0$ and ϕ_i in AFJJA in the presence of a 2π -fluxon. The self-induced magnetic field of the AF ground state has been subtracted from $2\pi\Phi_i/\Phi_0$. We find that a 2π -fluxon is unstable in the AFJJA and *fractionalizes into two spatially separated fluxons*, each carrying half the quantum of flux. Also, each of the *fractional fluxons is a π -kink* in ϕ_i . The magnetic field around the fractional fluxon decays as $\exp(-x/\lambda_{eff})$ where $\lambda_{eff} \approx 2\lambda_J$. This should be compared with the 2π -fluxon in the 0-JJA [Fig. 2(b)] where $\lambda_{eff} \approx \lambda_J$. The increase in λ_{eff} in AFJJA is a consequence of the magnetic flux in the AF ground state.

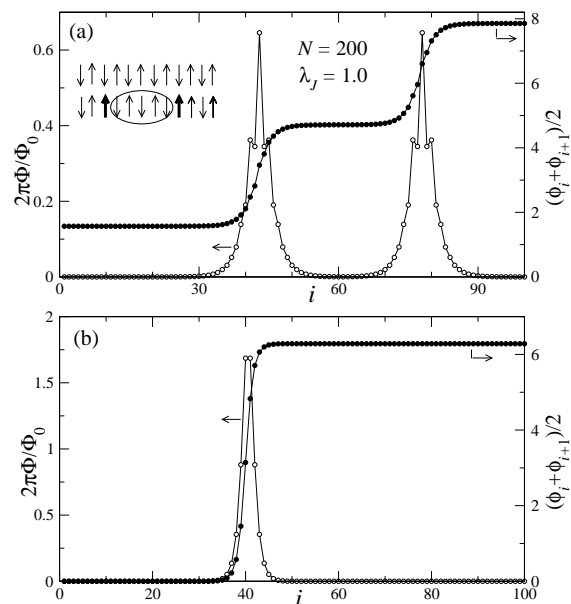


FIG. 2: (a) The magnetic flux $2\pi \frac{\Phi_i}{\Phi_0}$ and the average phase profile along the array in (a) AFJJA and (b) 0-JJA, in the presence of a 2π -fluxon. The background AF ground state has been subtracted from $2\pi \frac{\Phi_i}{\Phi_0}$ in (a). The schematic in inset (a) shows how the fractional fluxons (thick arrows) interpolate between the two degenerate ground state of Φ_i 's.

It is possible to vary the magnitude of the magnetic flux in each fraction by changing $i_c^* = I_c^\pi / I_c^0$ where I_c^π and I_c^0 are the critical currents of the π and 0 junctions,

respectively[20]. Figure 3(a) shows the spatial profile of the fractional fluxons for $i_c^* = 0.8$ and $\lambda_J = 1.0$. The phase change across the fractional fluxons is *not* π but is dependent on the value of i_c^* . The total phase change across both the fractions is always 2π , as required by the flux conservation. Figure 3(b) shows the magnitude of the integrated flux $2\pi\frac{\Phi_T}{\Phi_0}$ in each fractional fluxons as a function of i_c^* for $\lambda_J = 1.0$. The fractionalization occurs for $i_{cl}^* < i_c^* < i_{cu}^*$, where i_{cl}^* and i_{cu}^* are the two critical values. The slope $\frac{d\Phi_T}{di_c^*}$ at the critical values i_{cl}^* and i_{cu}^* appears to diverge, suggesting a transition between the fractionalized state and the single fluxon state. In experiments, the magnitude of the flux at the center of the fluxon Φ_m can be measured more easily. Figure 3(b) shows the behavior of $\Phi_m(i_c^*)$.

In Fig. 4, we show the numerically obtained parameter space λ_J - i_c^* . We have assumed that i_c^* can be varied independent of λ_J . The region of fractional fluxons is bounded by $i_{cl}^*(\lambda_J)$ and $i_{cu}^*(\lambda_J)$. It is easy to understand the absence of fractional fluxons in the limit $i_c^* \rightarrow 0$ since the array becomes a 0-JJA (with lattice constant twice the original array) which allows only 2π -fluxons. In the opposite limit $i_c^* \rightarrow \infty$ such that $I_c^0 \rightarrow 0$ and I_c^π is finite, there are two π junctions in each cell and the array can be shown to be equivalent to the 0-JJA, and the fractionalization is again not expected. In obtaining the parameter space in Fig. 4, I_c^0 is assumed to be finite and fixed which leads to fractionalization for $\lambda_J < 0.7$ even as $i_c^* \rightarrow \infty$.

The simulation results discussed above can also be understood analytically. Consider the case of $i_c^* = 1$. Define

$$\phi_{2m+1} = u_m, \quad \text{and} \quad \phi_{2m} = v_m, \quad (3)$$

where $m = 0, \frac{N}{2} - 1$. Thus, u_m and v_m are the gauge invariant phase differences across the π and 0 junctions, respectively. In the absence of any external fluxon, the u_m and v_m are invariant on translation by the lattice vector along the array. Hence, substituting $u_m = u$ and $v_m = v$, Eq.(2) becomes

$$\sin u = \sin v = 2\lambda_J^2(u - v). \quad (4)$$

There are two trivial solutions of the Eq.(4): $u = v = 0$ and $u = v = \pi$. The non-trivial solution of Eq.(4) is given by

$$u = \pi - v, \quad \text{and} \quad \sin v = 2\lambda_J^2(\pi - 2v). \quad (5)$$

For a given value of λ_J , the quantities v and u can be calculated graphically from Eq.(5). It can be easily verified that the non-trivial solution is the ground state for any finite λ_J . The magnetic flux in the cell is given by $\Phi = \pm(u - v)\frac{\Phi_0}{2\pi}$, where the + and - sign is for the cell to the left and the right of the π junction, respectively. Thus, the magnetic flux alternates in sign along the array. The values of u , v and $|\Phi|$ obtained from

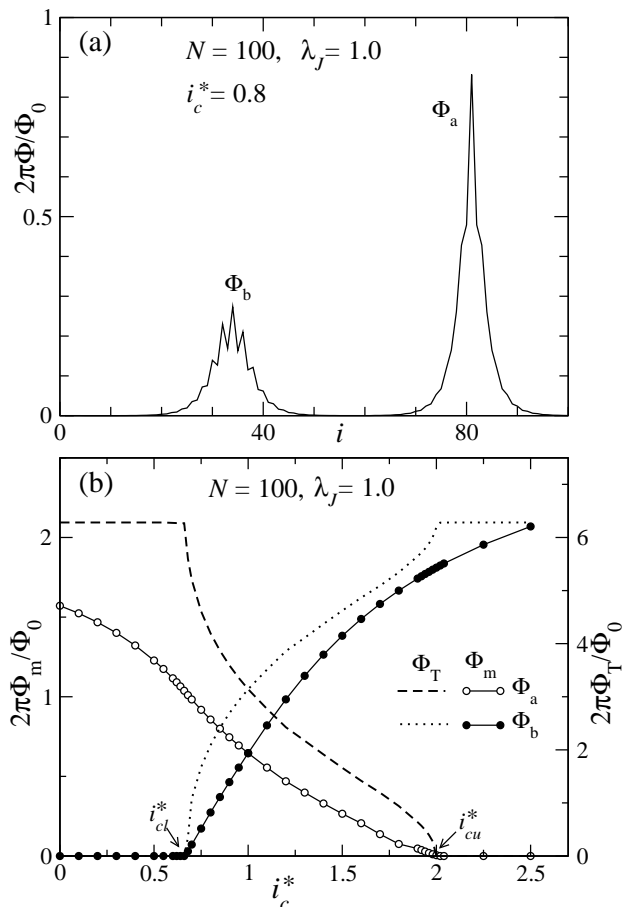


FIG. 3: (a) The spatial profile of the fractionalized external fluxon for $i_c^* = 0.8$ and $\lambda_J = 1.0$. The magnitude of flux in the two fractions are not equal. (b) The integrated total flux $2\pi\frac{\Phi_T}{\Phi_0}$ in the two fractional fluxons (represented by dashed and dotted lines) as a function of $i_c^* = I_c^*/I_c^0$. Also shown is the maximum flux $2\pi\frac{\Phi_m}{\Phi_0}$ at the center of the two fractional fluxons Φ_a and Φ_b (represented by symbols).

Eq.(5) are in excellent agreement with the numerically obtained values. In the strong screening limit $\lambda_J \rightarrow 0$, $u = \pi$ and $v = 0$, and the flux in each cell attains the maximum value $\Phi_0/2$. In the limit $\lambda_J \rightarrow \infty$, the solution of Eq.(5) is $u = v = \pi/2$ which is degenerate to the trivial solutions of Eq.(4), and the ground state contains no spontaneous magnetic flux.

To understand the fractionalization of a 2π -fluxon, we note that the AF ground state solution of Eq.(4) is two-fold degenerate. If $\phi = \{u, v\}$ obtained from Eq.(5) is one solution, the other solution is obtained by translating ϕ by one lattice constant. Thus, the other solution is $\phi' = \{u', v'\}$, where $u' = v + \pi$ and $v' = u + \pi$. The degeneracy of the ground state has an important implication: the elementary excitation for the array is a kink (or domain wall) in ϕ_i which interpolates between the two degenerate ground states ϕ and ϕ' . It can be easily verified that the phase change across the 'kink' is π and corresponds to an additional flux $\Phi_0/2$ in the array.

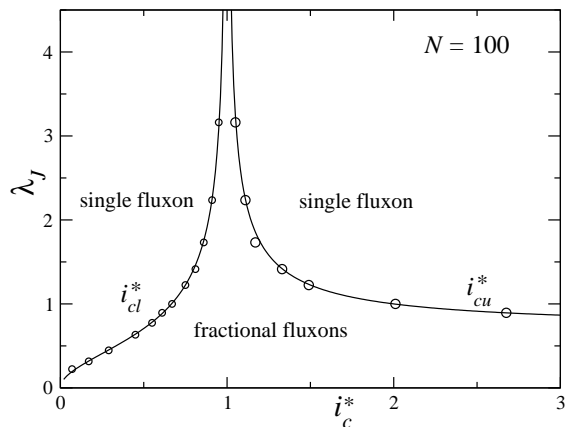


FIG. 4: The parameter space λ_J - i_c^* . The circles are the numerically obtained values whereas the full lines are the analytical result.

In the presence of a 2π fluxon, the energy minimization leads to two π -kinks which are separated by the degenerate ground states. This is shown schematically in the inset of Fig. 2(a). Fractionalization of a 2π fluxon in AFJJA is thus a consequence of the degeneracy of the ground state. A similar phenomenon is observed in polyacetylene [21] and certain field theories [22, 23] where fractional topological excitations occur and are related to the ground state degeneracy.

Equations (4) and (5) can be extended for the case $i_c^* \neq 1$. We find that the AF ground state is stable and fluxon fractionalization occurs for $i_c^* > 1$ when $\lambda_J < \lambda_{Ju} = \frac{1}{\sqrt{2}}(1 - \frac{1}{i_c^*})^{-1/2}$, and for $i_c^* < 1$ when $\lambda_J < \lambda_{Jl} = \frac{1}{\sqrt{2}}(\frac{i_c^*}{1-i_c^*})^{1/2}$. This is plotted in Fig. 4 and is in good agreement with the numerically obtained behavior of $i_{cu}^*(\lambda_J)$ and $i_{cl}^*(\lambda_J)$. Further details of the analytical calculations will be given elsewhere.

Next, we study the dynamical properties of the AFJJA. We restrict the analysis to the case $i_c^* = 1.0$ and in the absence of any external fluxon. The V - I curve is obtained by sweeping γ in small steps, and calculating $V = \alpha \langle \frac{d\phi}{dt} \rangle$ in the steady state (V is in units of $R_n I_c$). Recall that for the 0-JJA, all junctions switch from the superconducting state to the normal state simultaneously at $\gamma = 1$. In the AFJJA, the magnetic flux in the ground state alters this behavior significantly.

Figure 5 shows the V - I curve for $N = 30$ and $\lambda_J = 1$. The $\alpha = 0.1$ for the rest of the discussion below [24]. The important feature of the V - I curve is the appearance of a plateau in V above a depinning current γ_c . The transition to the normal state occurs at a higher current γ_n . By analyzing the spatio-temporal dynamics of fluxons on the voltage plateau, we find that the interpenetrating lattice of the flux (Φ) and the antflux ($-\Phi$) move in the opposite directions which appears as a stationary wave of breathing flux-antiflux pairs [25]. This is evident from the 2D space-time plot of $2\pi \frac{\Phi_i}{\Phi_0}$ which is shown for

a section of the array in the inset of Fig. 5. The $\frac{\Phi}{\Phi_0}$ in each cell oscillates between the positive and the negative values, and is in antiphase with the neighboring cells. Thus, at any instant of time, the total flux in the array is zero as expected from the ground state. We also find that for $\lambda_J > 1$, a linear flux flow regime appears before the plateau, whereas for small λ_J , the V shows a sharp step as shown in the inset of Fig. 5. The λ_J dependence of the width of the voltage plateau $(\Delta\gamma)_s = \gamma_n - \gamma_c$ is shown in Fig. 6(a). The $(\Delta\gamma)_s$ is non-monotonic and is maximum for $\lambda_J \approx 2$. Below a cut-off $\lambda_J^* \approx 0.45$, the plateau in V disappears and $\gamma_c = \gamma_n$.

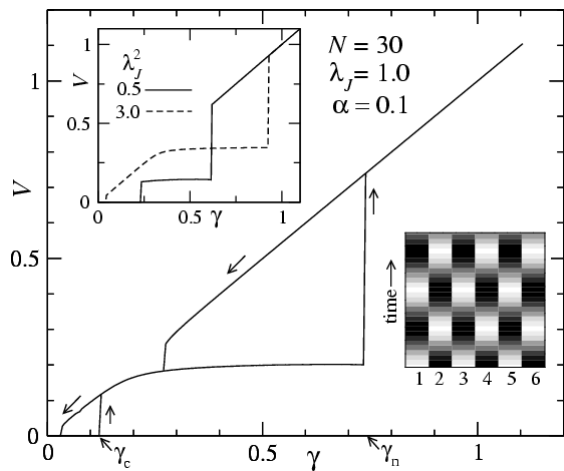


FIG. 5: The full V - I curve of the AFJJA. The direction of the current ramp is indicated by the arrow. Upper inset: the V - I curves for different values of λ_J (the V branch with increasing γ is shown). Left inset: the 2D space-time plot of $2\pi \frac{\Phi_i}{\Phi_0}$ in six cells of the array for $\gamma = 0.3$, where the maximum value is 2.2 (black) and the minimum value is -2.2 (white).

The origin of the plateau (or step) in V can be understood from the fluxon dynamics. In a 0-JJA, the motion of a single 2π -fluxon leads to the emission of small amplitude linear waves (plasma waves) due to the discreteness of the array. The resonances between these linear waves and the periodic motion of the fluxon causes a series of plateaus in V [17]. Extending this to the case of AFJJA, the plateau in V - I can be attributed to the phase locking between the moving fluxon lattice and the linear waves emitted by the array. The frequency ω_s of the linear waves can be calculated from Eq. (2). In the absence of any external fluxon, the symmetry of the ground state allows only waves with the wavevector $k = 2\pi/(2a)$ to be coupled resonantly to the moving fluxon lattice (here a is the lattice constant). Thus, all 0 and π junctions oscillate with the same amplitude and phase. Linearizing Eq.(2) for the π and the 0 junctions using $u = u_0 \exp(i\omega_s t)$ and $v = v_0 \exp(i\omega_s t)$, respectively,

$$\begin{aligned} -\omega_s^2 u - u &= 2\lambda_J^2 (v - u), \\ -\omega_s^2 v + v &= 2\lambda_J^2 (u - v). \end{aligned} \quad (6)$$

For simplicity, we have used $\alpha = \gamma = 0$. Adding the above equations gives the relation between u and v , $u = v(1 - \omega_s^2)/(1 + \omega_s^2)$. Substituting for u in the second equation leads to

$$(1 - \omega_s^2)(1 + \omega_s^2) + 4\lambda_J^2\omega_s^2 = 0. \quad (7)$$

The above quadratic equation in ω_s^2 can be solved to obtain the frequency of the linear waves

$$\omega_s(\lambda_J) = \sqrt{2\lambda_J^2 + \sqrt{1 + 4\lambda_J^4}}. \quad (8)$$

The ω_s is in units of the plasma frequency ω_P . The condition for phase locking of the linear waves with the moving fluxon lattice then becomes $\omega_s T = 2\pi$, where T is the time period corresponding to the motion of the fluxon lattice. From the simulation, the T (and hence ω_s) on the plateau can be obtained from the time evolution of the magnetic flux $\Phi_i(t)$ in a cell. In Fig. 6(b), the ω_s calculated analytically is compared with that obtained from the simulation for increasing λ_J . A reasonable agreement is observed over a range of λ_J . The discrepancy appears as λ_J approaches λ_J^* below which the plateau in V is not observed. The voltage V_s on the plateau is given by $V_s = \alpha\omega_s$. This is shown in Fig. 6(c) and is in good agreement with the simulation.

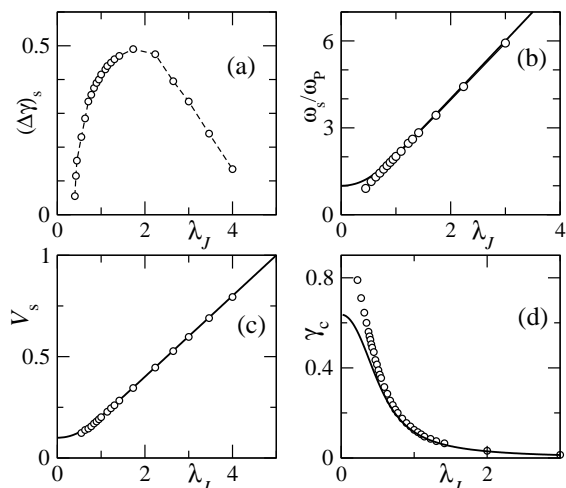


FIG. 6: (a) The λ_J dependence of the width of the voltage plateau $(\Delta\gamma)_s$. (b) Resonance frequency $\omega_s(\lambda_J)$, and (c) the voltage $V_s(\lambda_J)$. (d) The depinning current γ_c . The open symbols are from the simulation whereas the bold lines in (b), (c) and (d) are the analytical results described in the text.

Finally, the dependence of γ_c on the screening strength is shown in Fig. 6(d). A finite γ_c in JJA is attributed to the pinning potential created at the center of the cell [26]. For AFJJA, the pinning potential or the energy barrier can be defined as $\Delta E = E_M - E_A$, where E_M is the energy of the array with the fluxon lattice placed on the junctions and E_A is the ground state energy. Equating

the pinning force $2\Delta E$ to the Lorentz force required to overcome the energy barrier gives the depinning current γ_c (per junction),

$$\gamma_c = \frac{1}{\pi} \left(2 \cos(v) - \frac{1}{2} \lambda_J^2 (\pi - 2v)^2 \right). \quad (9)$$

The phase v in the above equation is the solution of the Eq.(5). Fig. 6(d) compares the above expression with the γ_c obtained from the simulation. The agreement is good at large λ_J , and the deviation appears as $\lambda_J \rightarrow \lambda_J^*$ below which no flux flow is observed.

In conclusion, we have introduced a new class of JJA containing π junctions. We considered the one-dimensional case in which every alternate junction is a π junction, and studied its properties numerically and analytically. The ground state of the array contains spontaneous magnetic flux in each cell and are ordered anti-ferromagnetically along the array. A 2π -fluxon in such an array is unstable and fractionalizes into two spatially separated π -fluxons. The fractionalization is related to the ground state degeneracy. The V - I curve shows a voltage plateau due to resonant interaction between the linear waves emitted by the array and the moving anti-ferromagnetic fluxon lattice present in the ground state.

Acknowledgments : Part of this work was done during the authors stay at the University of California, Davis.

Note : After the completion of the work, we became aware of the experimental fabrication of an array of coupled π -loops using YBaCuO-Nb zigzag structure in Ref.[27]. Some of the results obtained in this paper are applicable for such structures also. We thank the referees for bringing this paper to our attention.

* Electronic address: mchandran@tifr.res.in

† Electronic address: rahul@nec-labs.com

‡ Present Address: NEC Labs, 4 Independence Way, Princeton, NJ 08540.

- [1] A. F. Morpurgo, T. M. Klapwijk, and B. J. van Wees, *Appl. Phys. Lett.* **72**, 966 (1998).
- [2] A. F. Volkov, *Phys. Rev. Lett.* **74**, 4730 (1995).
- [3] F. K. Wilhelm, G. Schön, and A. D. Zaikin, *Phys. Rev. Lett.* **81**, 1682 (1998).
- [4] J. J. A. Baselmans, A. F. Morpurgo, B. J. van Wees, and T. M. Klapwijk, *Nature* **397**, 43 (1999); J. J. A. Baselmans, B. J. van Wees, and T. M. Klapwijk, *Phys. Rev. B* **63**, 094504 (2001).
- [5] R. Shaikhaidarov, A. F. Volkov, H. Takayanagi, V. T. Petrashov, and P. Delsing, *Phys. Rev. B* **62**, R14649 (2000).
- [6] The π junctions have been made also by coupling two superconductors across a ferromagnetic layer, see V. V. Ryazanov, V. A. Oboznov, A. Yu. Rusanov, A. V. Veretennikov, A. A. Golubov, and J. Aarts, *Phys. Rev. Lett.* **86**, 2427 (2001).
- [7] J. J. A. Baselmans, B. J. van Wees, and T. M. Klapwijk, *cond-mat/0107292* (2001).

- [8] F. V. Kusmartsev, Phys. Rev. Lett. **69**, 2268 (1992). See also L. N. Bulaevskii, V. V. Kusii, and A. A. Sobyenin, Pis'ma Zh. Eksp. Teor. Fiz. **25**, 314 (1977) [JETP Lett. **25**, 290 (1977)].
- [9] R. G. Mints, Phys. Rev. B **57**, R3221 (1998); R. G. Mints and I. Papiashvili, Phys. Rev. B **62**, 15214 (2000).
- [10] E. Goldobin, D. Koelle, and R. Kleiner, Phys. Rev. B **66**, 100508(R) (2002).
- [11] Mahesh Chandran, (unpublished).
- [12] R. V. Kulkarni, E. Almaas, K. D. Fisher, and D. Stroud, Phys. Rev. B **62**, 12119 (2000).
- [13] H. S. J. van der Zant, F. C. Fritschy, W. J. Elion, L. J. Geerligs, and J. E. Mooij, Phys. Rev. Lett. **69**, 2971 (1992). See also A. van Oudenaarden, S. J. K. Várdu, and J. E. Mooij, Phys. Rev. Lett. **77**, 4257 (1996) for localization, and A. van Oudenaarden and J. E. Mooij, Phys. Rev. Lett. **76**, 4947 (1996) for superfluid to Mott-insulator transition in Josephson junction array.
- [14] W. J. Elion, J. J. Wachters, L. L. Sohn, and J. E. Mooij, Phys. Rev. Lett. **71**, 2311 (1993).
- [15] P. Barbara, A. B. Cawthorne, S. V. Shitov, and C. J. Lobb, Phys. Rev. Lett. **82**, 1963 (1999).
- [16] A. Barone and G. Paterno, *Physics and Applications of the Josephson Effect*, (Wiley, New York, 1982).
- [17] A. V. Ustinov, M. Cirillo, and B. A. Malomed, Phys. Rev. B **47**, 8357 (1993).
- [18] A. V. Ustinov, B. A. Malomed, and S. Sakai, Phys. Rev. B **57**, 11691 (1998) and references there in.
- [19] We refer the fluxon created by applying a magnetic field to the array as an external fluxon. The external fluxon must be distinguished from the self-induced fractional fluxons present in the ground state of the array which appears in the *absence* of an applied magnetic field.
- [20] For the simulation purpose, we consider $I_c^0 = 1$ and vary I_c^π .
- [21] W. P. Su, J. R. Schrieffer, and A. J. Heeger, Phys. Rev. Lett. **42**, 1698 (1979); Phys. Rev. B **22**, 2099 (1980).
- [22] R. Jackiw, and J. R. Schrieffer, Nucl. Phys. **190**[FS3], 253 (1981).
- [23] R. Rajaraman, cond-mat/0103366, (2001).
- [24] The value of α chosen here may be small for the 3-terminal π junctions which have been implemented so far. We have verified that this does not affect the qualitative features discussed in the paper. A more realistic case would be to consider different values of α for 0 and π junctions.
- [25] Breathing mode of a vortex-antivortex pair in long Josephson junction have been studied previously. See K. K. Likharev, *Dynamics of Josephson junctions and circuits*, (Gordon and Breach, Amsterdam, 1986).
- [26] C. J. Lobb, D. W. Abraham, and M. Tinkham, Phys. Rev. B **27**, 150 (1983). M. S. Rzchowski, S. P. Benz, M. Tinkham and C. J. Lobb, Phys. Rev. B **42**, 2041 (1990).
- [27] H. Hilgenkamp, Ariando, Henk-Jan H. Smilde, D. H. A. Blank, G. Rijnders, H. Rogalla, J. R. Kirtley, and C. C. Tsuei, Nature **422**, 50 (2003).